A Modern Ampelography: A Genetic Basis for Leaf Shape and Venation Patterning in Grape[1][C][W][OPEN]

Daniel H. Chitwood[2], Aashish Ranjan, Ciera C. Martinez, Lauren R. Headland, Thinh Thiem, Ravi Kumar, Michael F. Covington, Tommy Hatcher, Daniel T. Naylor, Sharon Zimmerman, Nora Downs, Nataly Raymundo, Edward S. Buckler, Julin N. Maloof, Mallikarjuna Aradhya, Bernard Prins, Lin Li, Sean Myles, and Neelima R. Sinha*

Department of Plant Biology (D.H.C., A.R., C.C.M., L.R.H., T.T., R.K., M.F.C., T.H., D.T.N., S.Z., N.D., N.R., J.N.M., N.R.S.) and National Clonal Germplasm Repository, United States Department of Agriculture-Agricultural Research Service (M.A., B.P.), University of California, Davis, California 95616; Institute for Genomic Diversity and Department of Plant Breeding and Genetics, Cornell University, Ithaca, New York 14853 (E.S.B.); Agricultural Research Service, Department of Agriculture, Ithaca, New York 14853 (E.S.B.); Biostat Solutions, Mt. Airy, Maryland 21771 (L.L.); and Department of Plant and Animal Sciences, Nova Scotia Agricultural College, Truro, Nova Scotia B2N 5E3, Canada (S.M.)

ORCID ID: 0000-0003-4875-1447 (D.H.C.).

Terroir, the unique interaction between genotype, environment, and culture, is highly refined in domesticated grape (*Vitis vinifera*). Toward cultivating terroir, the science of ampelography tried to distinguish thousands of grape cultivars without the aid of genetics. This led to sophisticated phenotypic analyses of natural variation in grape leaves, which within a palmate-lobed framework exhibit diverse patterns of blade outgrowth, hirsuteness, and venation patterning. Here, we provide a morphometric analysis of more than 1,200 grape accessions. Elliptical Fourier descriptors provide a global analysis of leaf outlines and lobe positioning, while a Procrustes analysis quantitatively describes venation patterning. Correlation with previous ampelography suggests an important genetic component, which we confirm with estimates of heritability. We further use RNA-Seq of mutant varieties and perform a genome-wide association study to explore the genetic basis of leaf shape. Meta-analysis reveals a relationship between leaf morphology and hirsuteness, traits known to correlate with climate in the fossil record and extant species. Together, our data demonstrate a genetic basis for the intricate diversity present in grape leaves. We discuss the possibility of using grape leaves as a breeding target to preserve terroir in the face of anticipated climate change, a major problem facing viticulture.

Grape (*Vitis* spp.) leaves possess five major veins in a palmate arrangement, the blade supported by a prominent petiole that positions the leaf for optimal light capture. Besides this consistency, all other characters of *Vitis* spp. leaves vary widely, exhibiting striking diversity (Galet, 1952). Leaves can be simple, dissected to the extent that they are compound, or possess any degree of lobing, in various shapes and forms, between these two extremes. The lengths and angles between the superior (distal) and inferior (proximal) lateral veins create an array of leaf morphs, including orbicular (circular), reniform (kidney shaped), and cordate (heart shaped). Leaves vary in their hirsuteness, color, surface contour, size, and dentation. Not only do leaves vary in morphology by genotype, but some cultivars exhibit profound heteroblasty, with complex shape trends within a shoot.

Perhaps the most unique aspect of grape leaves is not their profound morphological diversity but rather that this variation has been quantified to an unprecedented degree compared with other crops. Ampelography (Αμπελος, "vine" and γραφος, "writing") is the science of phenotypically distinguishing grapevines. The authoritative ampelographic reference is the *Précis d'Ampélographie Pratique* (Galet, 1952), translated into English as *A Practical Ampelography: Grapevine Identification* (Galet, 1979), which prominently features leaves (among other traits) for most domesticated and many wild vines. The impetus of many ampelographers was to unravel complex synonymous name relationships given to vines as they were transported between European countries with multiple languages. The singular focus to identify distinct genotypes was fueled by economics and the concept of terroir, that particular genotypes were better suited to different locations because of geology and climate. Another example of

[1] This work was supported by the Gordon and Betty Moore Foundation of the Life Sciences Research Foundation (to D.H.C.) and the National Science Foundation (grant no. IOS–0820854 to N.R.S. and J.N.M.).

[2] Present address: Donald Danforth Plant Science Center, St. Louis, MO 63132.

* Address correspondence to nrsinha@ucdavis.edu.

The author responsible for distribution of materials integral to the findings presented in this article in accordance with the policy described in the Instructions for Authors (www.plantphysiol.org) is: Neelima R. Sinha (nrsinha@ucdavis.edu).

[C] Some figures in this article are displayed in color online but in black and white in the print edition.

[W] The online version of this article contains Web-only data.

[OPEN] Articles can be viewed online without a subscription.

www.plantphysiol.org/cgi/doi/10.1104/pp.113.229708

the importance of ampelography was demonstrated during the Phylloxera crisis in late 19th century France (Mullins et al., 1992). Breeding experiments and grafting required precise knowledge of American and European vine identity. Of course, molecular genetics had yet to be discovered, and leaves were a prominent, distinguishing phenotypic feature of vines.

Here, we present a comprehensive ampelographic assessment of, and demonstrate a genetic basis for, leaf morphology in more than 1,200 varieties of grape. Elliptical Fourier descriptors (EFDs) of leaf outlines and Procrustes analysis of lobe tips, sinuses, and major vein branch points provide a global analysis of leaf shape. These quantitative traits correlate with the phenotypes measured by Galet (1952), suggesting a genetic component to leaf morphology measured across continents and decades. A meta-analysis of our data with previously measured traits demonstrates correlation between leaf shape and hirsuteness, linking morphology to an adaptive trait of the epidermis. The genetic basis of leaf morphology is reflected in high estimated heritability values for our traits and correlation with population structure, geography, and production use. RNA-Seq analysis of a complex leafed spontaneous mutant reveals down-regulation of meristem identity and leaf patterning genes as well as a commensurate up-regulation of oxidative stress pathways, indicating precocious senescence. Additionally, as a first step toward mapping the genetic basis of leaf morphology, we perform a genome-wide association study (GWAS). Together, our data demonstrate a strong genetic basis for leaf shape and quantitatively measure the extent of natural variation in grape. We discuss the grape leaf as a potential breeding target to combat the predicted effects of climate change on viticulture.

RESULTS

Morphometric Analysis of Leaf Shape

Although comprehensive, the ampelography of Galet (1952) is over half a century old, relying on trait measurements failing to encompass the entirety of shape and vein patterning in leaves. Additionally, the analysis was performed on grapevine collections for which dense genotyping is currently lacking. We sought to not only find a genetic basis for the intricate leaf morphs present in grape using the recently genotyped U.S. Department of Agriculture (USDA) germplasm collection (Winters, CA; Myles et al., 2011) but to use modern morphometric techniques, such as EFDs (Iwata et al., 1998; Iwata and Ukai, 2002; Chitwood et al., 2012b, 2012c, 2012d) and generalized Procrustes analysis (GPA) of leaf venation landmarks (Rohlf and Slice, 1990; Viscosi and Cardini, 2011), to globally quantify shape variation.

We measured multiple traits of four leaves from each of two vines representing more than 1,200 grapevine accessions (more than 9,500 measured leaves; Supplemental Data Sets S1 and S2). The diversity of leaf morphs present can be represented by the simple morphometric measures of circularity and aspect ratio (AR; Fig. 1). Circularity $[4\pi \times (\text{area} \div (\text{perimeter})^2)]$, a ratio of the area to perimeter of an outline, is sensitive to lobing and serration in the context of grape leaves. Varieties such as Champanel (DVIT2632) and Agawam (DVIT2630) have high circularity values and little lobing and entire (lacking serration) margins. Although classified as grape, these particular cultivars have a known parentage with contributions from both grape and wild *Vitis* spp. (Agawam possesses *Vitis labrusca* in its parentage and Champanel possesses *Vitis champinii* and *V. labrusca*), perhaps contributing to their extreme leaf shapes. Contrastingly, Ciotat (DVIT2107, DVIT0372) possesses leaves with extreme dissection to the point of being compound and has extremely low circularity values, reflecting the increased perimeter relative to blade area (Fig. 1). AR refers to the ratio of the major axis to the minor axis of a fitted ellipse. Leaves with AR values close to 1 are circular in shape, whether they possess lobing (Chasselas Dore, DVIT0373) or not (Agawam, DVIT2630). Because the best-fit ellipse is used, any deviation from a circular leaf morph increases AR

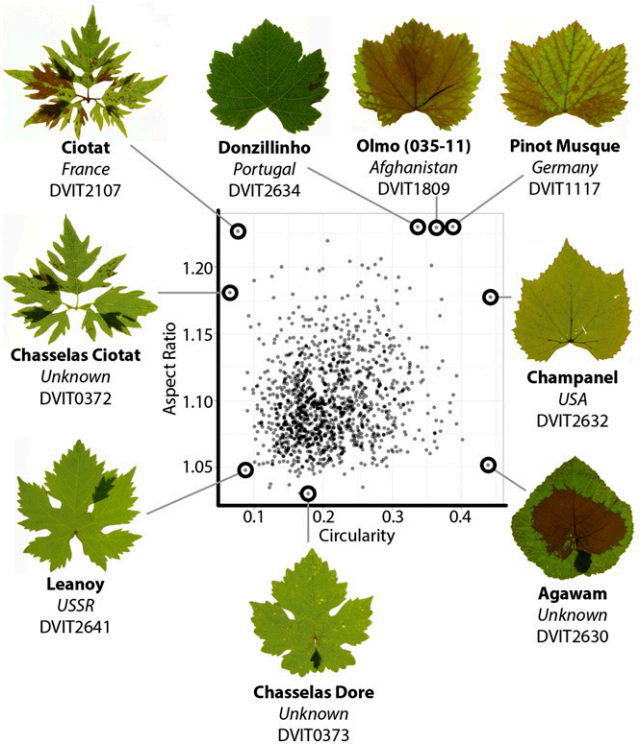

Figure 1. AR and circularity among grape accessions. Averaged AR (major/minor axis of a fitted ellipse) and circularity (the ratio of area to perimeter squared times 4π) values of 1,213 accessions in the USDA germplasm collection are shown. In this population, high AR values indicate leaves with low length-to-width ratios, and leaves with low circularity have increased lobing and serration. Leaves from accessions exhibiting extreme AR and circularity values are shown. In this and subsequent figures, the common name (boldface), place of origin (italics), and accession number (roman) of leaves is provided below the photographs. [See online article for color version of this figure.]

value, and most often in grape such deviation reflects increases in leaf width relative to length (e.g. Donzillinho, DVIT2634; Olmo [035-11], DVIT 1809; Pinot Musque, DVIT1117; Fig. 1).

The shape of grape leaves is influenced by much more than just lobing, serration, and AR. Grape leaves invariably possess a midvein (L_1), two superior (distal) lateral veins (L_2), two inferior (proximal) lateral veins (L_3), two petiolar veins that branch distally from the inferior lateral veins (L_4), and a prominent petiolar sinus (for diagram, see Fig. 4B). The angular distances between the major veins and the distinctness of the petiolar veins and sinus are some of the most distinguishing leaf characters used by Galet (1952) to differentiate grape varieties. To capture this shape information, which is not represented in circularity and AR, we performed an EFD analysis on leaf outlines (Fig. 2). Resulting shape principal components (PCs; prefixed by "sym" to denote that they explain "symmetrical" shape variance) from the analysis describe intuitive leaf shape qualities traditionally difficult to quantify. Low symPC1 values describe distinct lobing and spaced petiolar veins (Feteasca Neagra, DVIT 3255), whereas high symPC1 values describe a flattened leaf tip and a more enclosed petiolar sinus (Hosargoon, DVIT2503). Like low symPC1 values, low symPC2 values describe an archetypal leaf morph with prominent lobes (Gaschochi, DVIT2537), whereas high symPC2 values describe leaves with little lobing between the inferior and superior lateral veins and a prominent tip (Barlinka, DVIT0349). symPC3 to symPC5 describe shape variance relating to lobe distinctness and the prominence and shape of the petiolar sinus. Together, the five PCs analyzed in this work explain more than 80% of all shape variance measured (Fig. 2).

Procrustes Analysis of Venation Patterning

A relationship between vein patterning and leaf shape is obvious in grape. To a large extent, the positioning of lobes is determined by the placement of the superior (L_2) and inferior (L_3) lateral veins, and the shape of the petiolar sinus is determined by the branching angles of the petiolar (L_4) veins (Figs. 2–4). Such a relationship has been noted in other species (Dengler and Kang, 2001) and is not surprising considering the important role of auxin canalization in both vein (Scarpella et al., 2006) and leaf (Reinhardt et al., 2003; Koenig et al., 2009) patterning.

We took advantage of the regular morphology of grape leaves to perform a GPA based on venation

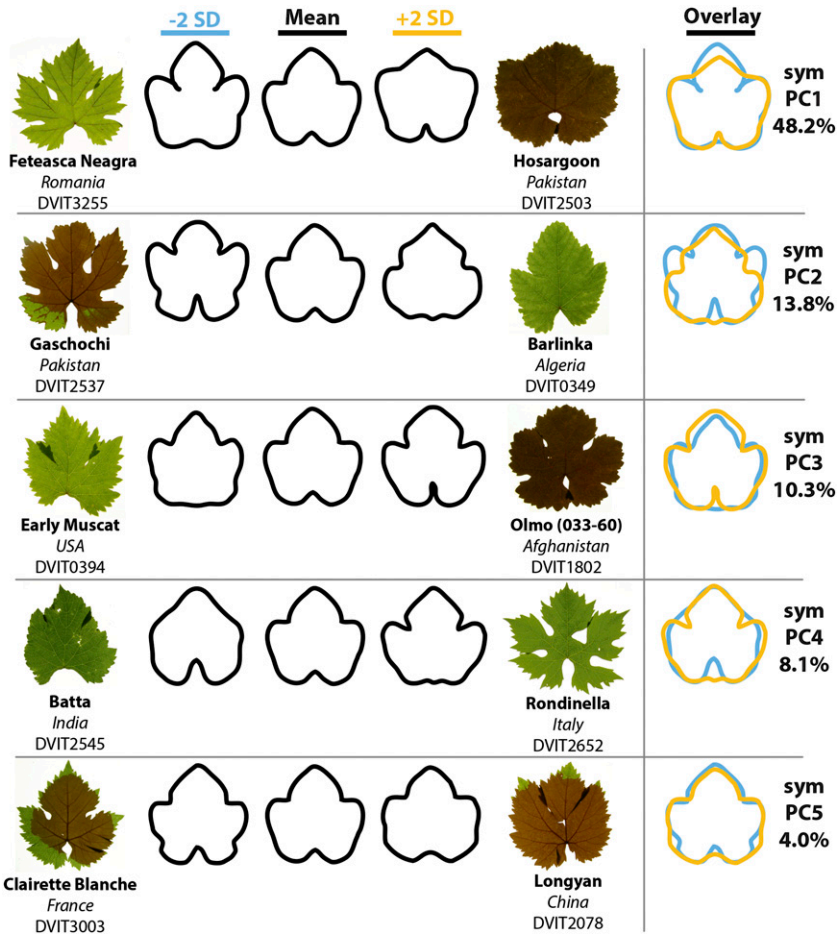

Figure 2. EFDs of symmetrical shape variation. Eigenleaves resulting from a PCA on EFDs derived from 9,485 leaves of 1,220 accessions are shown. Shown are the first five PCs and the percentage variation in symmetrical shape that they explain. For each PC, the eigenleaves at −2 (blue) and +2 (orange) SD along the PC axis are shown. An overlay of the eigenleaves at ±2 SD indicates the shape variance explained by each PC. Representative leaves of accessions with extreme PC values are shown. PCs resulting from the analysis of EFDs are indicated as symPC, referring to the symmetrical shape variance they explain. The five symPCs considered in this article explain 84.4% of all symmetrical shape variance analyzed.

landmarks. In the first analysis, 10 landmarks were used, including the tips of the midvein (L_1), superior (L_2) and inferior (L_3) lateral veins, superior (Si_s) and inferior (Si_i) sinus valleys, and the petiolar junction (Fig. 3A). PCs for these landmarks are called "outer" (denoted "oPC") because they fall on the margin of the leaf. This analysis is sensitive to lobing. oPC1 explains 33.6% of all variance, encompassing leaves that completely lack lobing (Red Ohanez, DVIT0499) and leaves so lobed that they are technically complex (Chasselas Ciotat, DVIT0372). oPC2 describes variance relating to lobes angled toward the tip of the leaf (Summer Royal, DVIT2899) versus those angled toward the base (Chasselas Rose, DVIT0376). oPC3 describes stretching along the horizontal axis of the leaf, as seen comparing the accession 5-20 (DVIT1980) with Muscat Noir (DVIT0469).

To analyze the branching pattern of leaf veins, we performed an "inner" analysis (denoted "iPC"). The midvein, superior, and inferior veins all have prominent branch points near the petiolar junction. Using the branch points as landmarks, patterns such as the proximity of the inferior vein branch points to each other and the distance of the midvein branch point from the petiolar junction can be discerned (iPC1; Fig. 3B). iPC2 explains variance relating to the separation of superior vein branch points and the proximity of the midvein branch point to the petiole (as seen in Niunai [DVIT2094], resulting in a "squished" appearance). The placement of the petiolar junction relative to the inferior branch points is explained by iPC3, describing the "low" petiolar junction of Ciotat (DVIT2107) compared with the "high" junction of Agawam (DVIT2630).

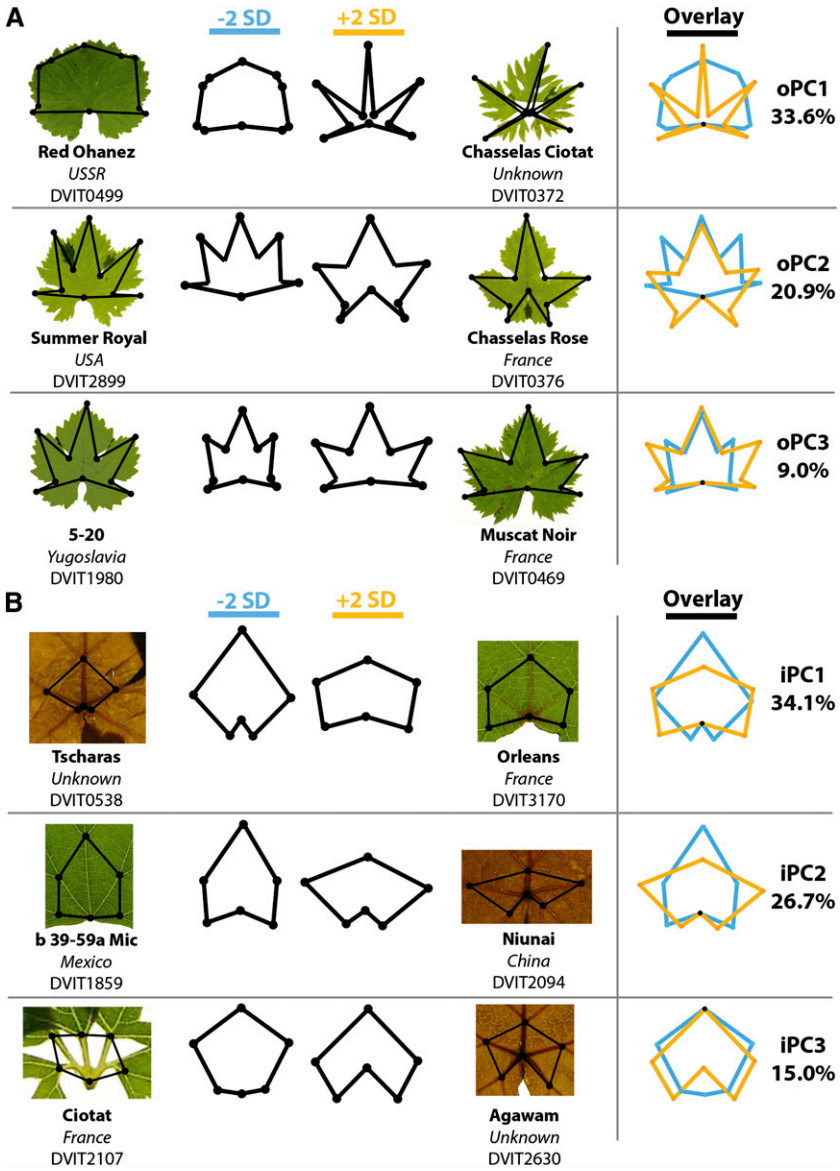

Figure 3. GPA of venation patterning. A, PCs resulting from a Procrustes analysis of "outer landmarks" (these PCs are indicated as oPCs). There are 10 landmarks in the outer analysis, including the petiolar junction, tip of the midrib (L_1), the tips of the left and right superior (distal; L_2) and inferior (proximal; L_3) lobes, and the left and right superior (Si_s) and inferior (Si_i) sinuses. For each PC, eigenleaves at −2 (blue) and +2 (orange) SD along the PC axis, the overlay of these leaves, and the percentage variation explained by the PC are given. Representative leaves from accessions with extreme values for each PC are shown. The three PCs analyzed in the outer analysis explain 63.5% of the variance in this data set. B, Similar to A, except showing PCs resulting from analysis of the "inner landmarks." There are six landmarks in the inner analysis, including the petiolar junction, branch point of the midrib (L_1), the left and right major branch points of the superior (L_2) lateral veins, and the left and right branch points between the inferior (L_3) and petiolar (L_4) veins. The three PCs analyzed in the inner analysis explain 75.8% of the variance in this data set. For visual descriptions of the midrib (L_1), superior lateral veins (L_2), inferior lateral veins (L_3), petiolar veins (L_4), and superior and inferior sinuses (Si_s and Si_i), see Figure 4B.

Correspondence of Traits with Those Measured by Galet and Heritability

Because leaf shape closely follows venation patterning, it is not surprising that many of our traits are significantly correlated (Fig. 4A; Supplemental Data Sets S3 and S4). Trait correlation reveals two intuitive groups of traits. The first (Fig. 4A, solid line box) is a constellation of traits explaining lobing and serration, including circularity (Fig. 1), symPC1 (Fig. 2), and oPC1 (Fig. 3A). The second (Fig. 4A, dotted line box) includes two subgroups, both of which relate to the angular placement of lobes. The first subgroup consists of traits explaining compactness and the roundness of a leaf, including AR (Fig. 1), symPC4 (Fig. 2), and iPC1 (Fig. 3B). The second subgroup includes traits relating to the placement of the petiolar junction relative to the branch points of the inferior lateral veins, including symPC3 (Fig. 2), oPC2 (Fig. 3A), and iPC3 (Fig. 3B).

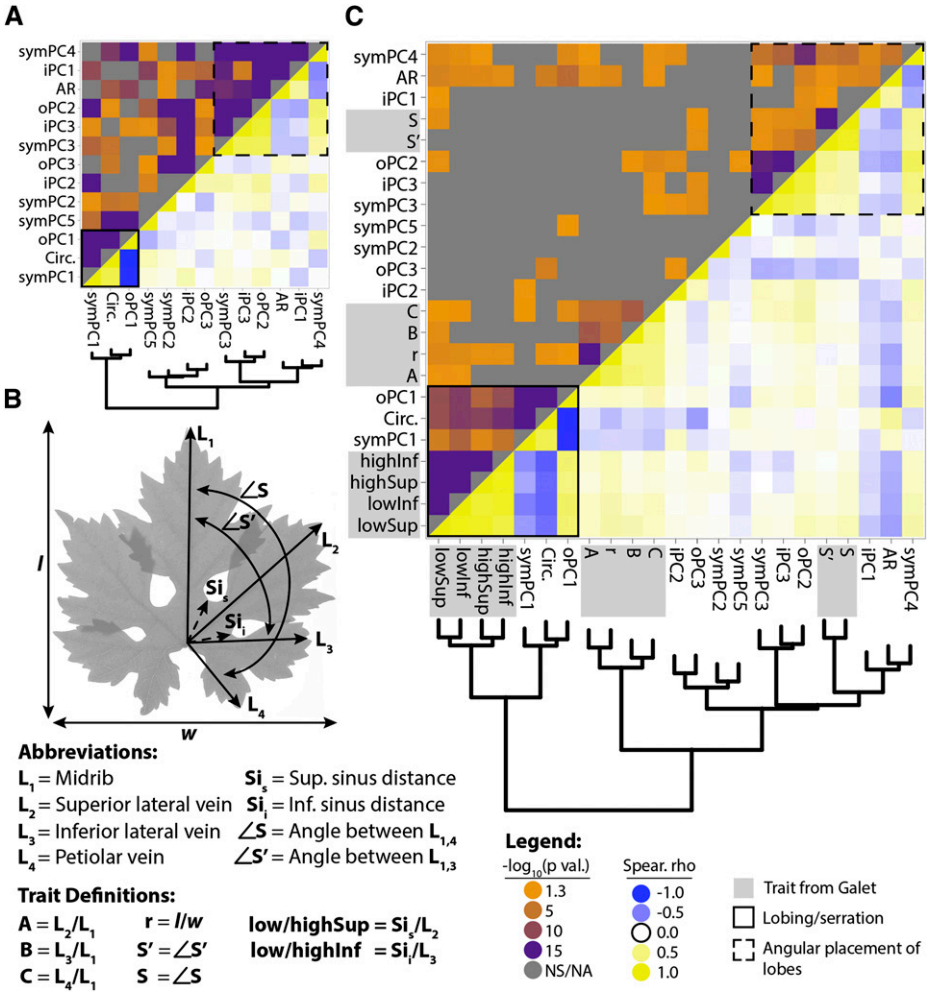

Figure 4. Correlation of traits with each other and with measurements from Galet (1952). A, Hierarchical clustering and heat map of the correlation of traits, as measured in 1,220 accessions, with each other. The top quadrant indicates correlation *P* values, and the bottom quadrant indicates Spearman's ρ. The solid line box indicates high correlation between symPC1, circularity, and oPC1, traits related to lobing and serration. The dashed line box indicates high correlation between symPC3, iPC3, oPC2, AR, iPC1, and symPC4, measures that are sensitive to the angular placement of the superior and inferior lateral veins to each other. B, Traits measured by Galet (1952, 1979). Measures of vein length (L_1–L_4), sinus distance (Si_s and Si_i), and angles between veins ($\angle S$ and $\angle S'$) are indicated and defined. r is length-to-width ratio; A, B, and C are ratios of vein lengths; S and S′ are angular distances between veins; and low/highSup and low/highInf are low and high estimates of superior and inferior lobing. C, Hierarchical clustering and heat map of the correlation of traits measured in this article with that of Galet (1952; indicated in light gray in the margins). Correlation is between 122 accessions matched between the USDA germplasm collection and Galet (1952). The solid line box indicates high correlation between the measures of Galet (1952) for lobing and measures of lobing and serration measured in this article. The dashed line box indicates high correlation between the measures of Galet (1952) for angular positioning of superior and inferior veins with similar traits measured in the USDA germplasm collection. *P* values are indicated in orange to purple (less to more significant) and gray (not significant [NS/NA]). Spearman's ρ is indicated in blue (negative), yellow (positive), and white (neutral).

Table I. *Heritability estimates of traits*

Estimates of the heritability of traits accounting for population structure and cryptic relatedness are as described by Yang et al. (2011). Provided are the trait, sample number, and heritability estimate.

Trait	*n*	h^2
oPC2	928	0.4594
symPC1	936	0.4321
symPC4	936	0.4285
oPC1	926	0.4222
iPC3	928	0.4184
iPC1	928	0.4064
Circularity	927	0.3949
iPC2	928	0.3936
symPC5	936	0.3415
symPC3	936	0.3144
oPC3	928	0.2303
AR	928	0.2277
symPC2	934	0.2162

Venation and leaf shape traits correlate because they describe leaf attributes influenced by similar underlying phenomena (e.g. auxin). Similarly, completely different measures of leaf morphology would be expected to correlate with our measurements as well. We sought to determine whether the leaf traits of Galet (1952) correlate with our measurements.

The measurements of Galet (1952) include vein lengths (L_1–L_4) and their ratios (A, B, C), sinus depth (low/highSup, low/highInf), and angular differences between veins (S and S′; Fig. 4B). To ensure that we were comparing correct genotypes, we collected the measurements of Galet (1952) for 122 cultivars with unambiguous name/synonym matches to the USDA germplasm (Supplemental Data Set S5). The clustering of our trait measurements together with those of Galet (1952) demonstrates the robustness of the two main trait categories mentioned previously (Fig. 4C; Supplemental Data Sets S6 and S7). The measurements of Galet (1952) for sinus depth (low/highSup, low/highInf) cluster most closely with our measures of lobing and serration (Fig. 4C, solid line box), whereas the measurements of Galet (1952) for angular distance (S and S′) most closely associate with our constellation of traits relating to lobe and vein positioning (Fig. 4C, dotted line box).

The significant correlation between our traits and those of Galet (1952) is highly suggestive of an important genetic component underlying leaf morphology in *Vitis* spp. The measurements of Galet (1952) were not only

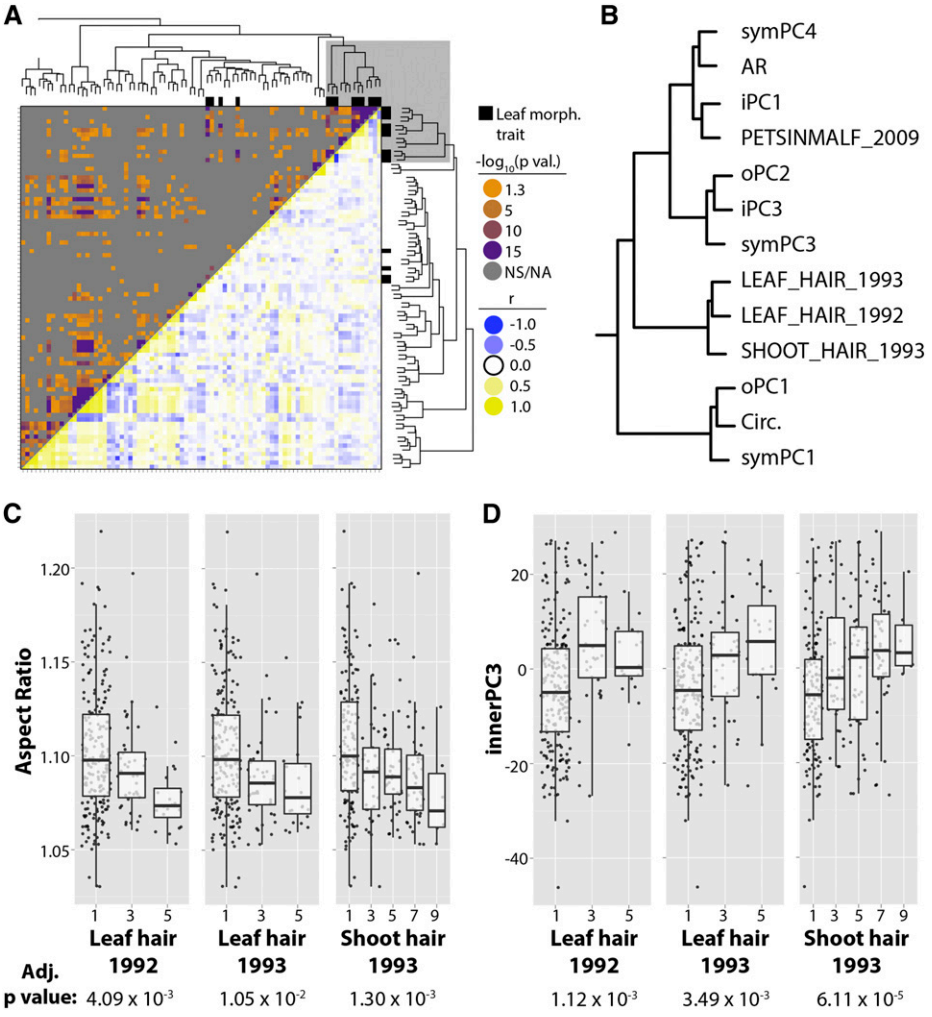

Figure 5. Meta-analysis of traits with data from GRIN. A, Hierarchical clustering and heat map of the correlation of traits with those present in GRIN. Seventy-five GRIN traits (representing 36 distinct phenotypes measured in multiple years at the USDA germplasm collection) are hierarchically clustered with traits measured in this article. Most traits measured in this article (black rectangles) cluster together (gray box). *P* values are indicated in orange to purple (less to more significant) and gray (not significant, [NS/NA]). r is length-to-width ratio, indicated in blue (negative), yellow (positive), and white (neutral). B, Closeup of the gray box in A. Traits relating to the angular placement of the superior and inferior veins correlate most closely with trichome density (LEAF_HAIR and SHOOT_HAIR) and shape of the petiolar sinus (PETSINMALF). C and D, Significant correlations of AR (C) and iPC3 (D) with GRIN leaf and shoot trichome densities shown as box plots superimposed upon jittered values. FDR-controlled *P* values for correlations are provided.

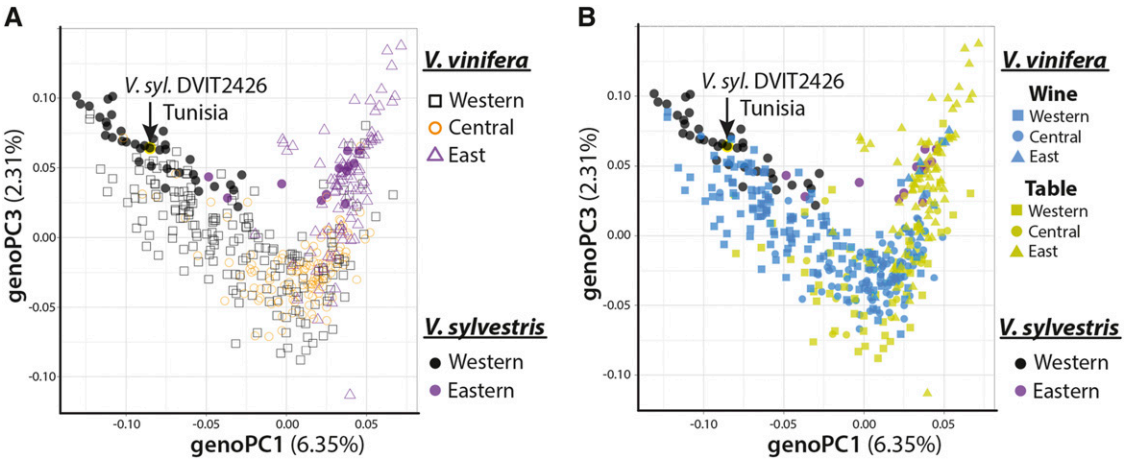

Figure 6. Population structure of grape and *V. sylvestris* accessions. PCA results reflect the population structure in wild and domesticated grape. Genotypic PCs are referred to as genoPCs to distinguish them from other trait PCs used in this article. Graphs of genoPC1 and genoPC3 (explaining 6.35% and 2.31% of genotypic variation, respectively) with grape accessions colored by point of origin (A; western, black; central, orange; eastern, magenta) and by production type (B; wine, blue; table, yellow) are shown. In both graphs, western and eastern *V. sylvestris* accessions are indicated by black and magenta, respectively. genoPC1 and genoPC3 are shown because of their prominent correlations with traits. Note that genoPC1 explains the eastern versus western population structure, whereas genoPC3 explains the central-specific patterns of variance. The *V. sylvestris* accession DVIT2426 that was sampled is indicated.

made on different vines but over half a century ago on a different continent, and correlation demonstrates genetic influences predominating over substantial environmental differences.

To formally demonstrate the heritability of leaf shape in grapevines, we estimated heritability values for our traits using a genomic partitioning method that accounts for variance attributable to population structure and cryptic relatedness (Table I; Yang et al., 2011). Nearly half of our traits are estimated to have relatively high heritability ($h^2 \geq 0.4$), whereas the remainder possesses heritability of intermediate values ($0.2 < h^2 < 0.4$). High heritability in leaf dimensions (Tian et al., 2011) and leaf shape (Langlade et al., 2005; Chitwood et al., 2013) has been demonstrated in maize (*Zea mays*), *Antirrhinum* spp., and tomato (*Solanum lycopersicum*). Here, we demonstrate in *Vitis* spp. that vascular patterning, in addition to leaf shape, is a highly heritable attribute of leaf morphology as well.

The Phenotypic Context of Leaf Shape: a Special Relationship with Berries and Hirsuteness

Leaves are not just the major photosynthetic organs in plants. As the default archetype from which other organs are derived (Goethe, 1817; Friedman and Diggle, 2011), the developmental genetic programs that regulate leaf shape can globally impact the morphology of lateral organs throughout a plant. Because of the central importance of leaves, natural variation in leaf shape can constrain phenotypes in disparate organs. For example, we previously have shown in tomato a relationship between leaf shape and sugar levels in the fruit. This relationship arises through either shared developmental pathways between leaves and the berry or indirect effects on photosynthetic efficiencies imparted by different leaf morphs (Chitwood et al., 2013). Likewise, how does the shape of leaves fit into the larger phenotypic context of grapevines?

We assembled 36 distinct phenotypes, measured in multiple years (amounting to 75 traits), from the USDA Germplasm Resources Information Network (GRIN; Supplemental Data Set S8). At minimum, 117 vines were measured for each trait. Correlation of GRIN traits with our traits and each other (Supplemental Data Sets S9 and S10) and subsequent hierarchical clustering (Fig. 5A) reveals that leaf morphology phenotypes are highly self-correlative (Fig. 5A, gray box). A few of our leaf shape traits cluster out of this constellation, including symPC2, oPC3, and iPC2 (Supplemental Fig. S1, yellow box). These traits are related to the angular placement of the distal (L_2) and proximal (L_3) lateral veins (Figs. 2 and 3) but more importantly explain variation in which the close proximity of these veins all but eliminates the inferior sinus cavity (Si_i; Fig. 4B). Importantly, these traits closely associate with another morphological feature, the lack of blade outgrowth beyond the petiolar veins along the sinus rim (so-called "naked veins"; Supplemental Fig. S1). These aspects of leaf shape are associated with Brix in berries and other important fruit attributes, including flavor, véraison, and seedlessness (Supplemental Fig. S1). Considering that much of the sugar in mature berries is ultimately derived from leaf photosynthate (Davies and Robinson, 1996), these results are consistent with the hypothesis that leaf shape can impact photosynthesis and, therefore, berry sugar accumulation, as proposed originally in tomato (Chitwood et al., 2013).

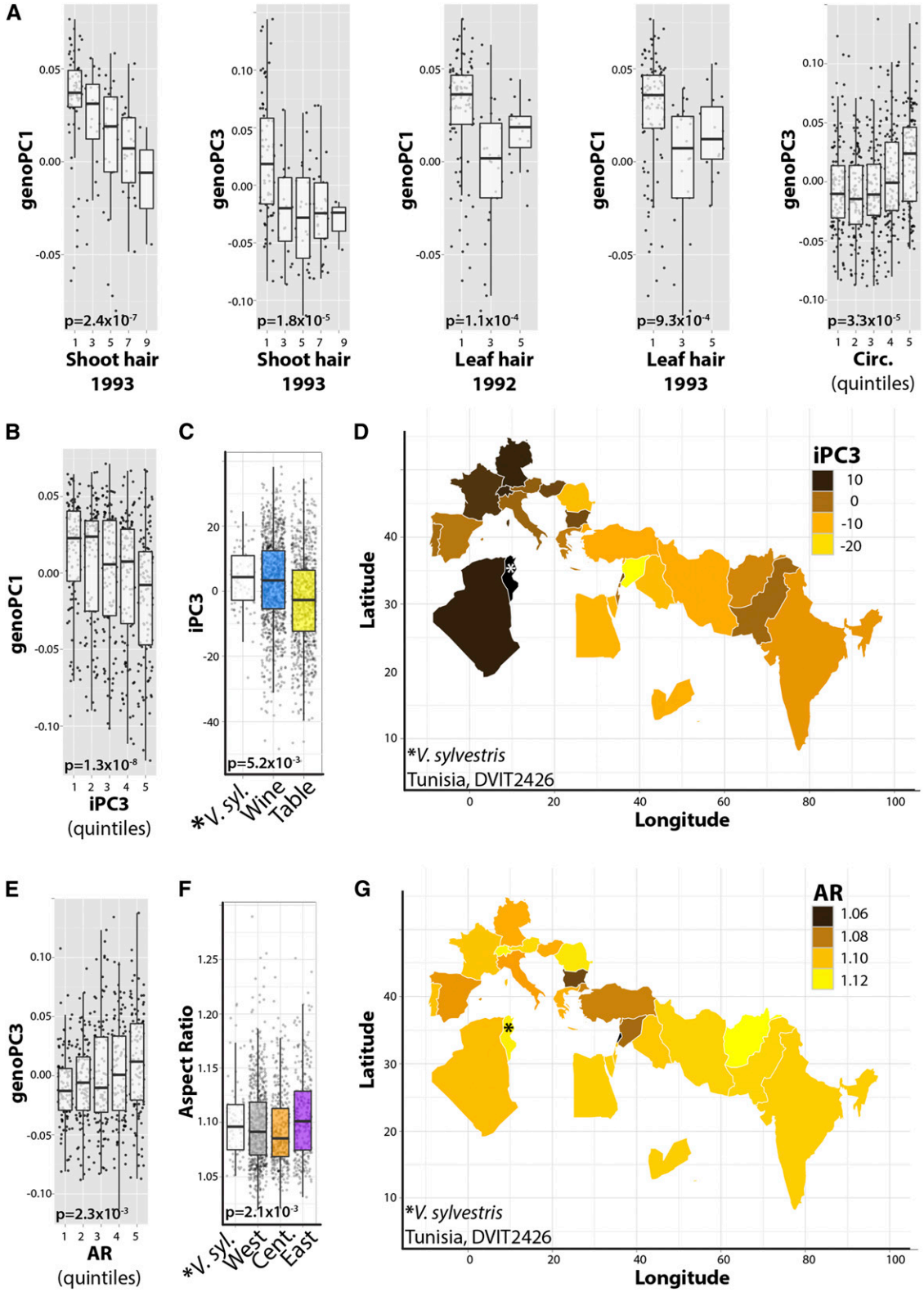

Figure 7. Correlations between traits and genotypic PCs. A, Box plots of significant correlations between genoPC1 and genoPC3 with GRIN measures of trichome density and leaf circularity. Bonferroni-corrected *P* values are provided. B to G, iPC3 (B–D) and AR (E–G) are two traits that correlate not only with genoPCs (genoPC1 and genoPC3, respectively) but also with production type and geographical attributes of accessions (iPC3 with production type and AR with geography). For genoPC1/iPC3 and genoPC3/AR, correlations between the genoPC and trait are provided, as well as differences by production type and

The most prominent relationship between leaf morphology with other traits is hirsuteness (Fig. 5B). Both traits relating to the angular placement of lateral veins (Fig. 4, A and C, dotted line square) and lobing and serration (Fig. 4, A and C, solid line square) associate closely with the density of trichomes on leaves and shoots (Fig. 5, B–D). Also included among this group of traits is the shape of the petiolar sinus (Fig. 5B, PETSNIMALF), which associates with other measures of angular vein positioning.

The correlation of leaf trichome density with leaf shape links macromorphological and micromorphological features of the leaf, a relationship rarely described (McLellan, 2005). That intricate aspects of laminar outgrowth, vein patterning, and epidermal features track each other among domesticated grape cultivars is suggestive that these traits are regulated by common developmental pathways. That this suite of leaf traits could be altered together during evolution has interesting implications for the adaptive significance of leaf morphology. Leaf shape mirrors precipitation and temperature in the fossil record (Bailey and Sinnott, 1915; Wolfe, 1971; Greenwood, 1992; Wilf et al., 1998; Chitwood et al., 2012a), environmental factors closely associated with the function of trichomes in boundary layer maintenance, thermoregulation, and leaf surface reflectance, all factors critical for the photoprotection of grape leaves (Liakopoulos et al., 2006).

Population Structure and Leaf Morphology

As described previously, the genetic structure of grape populations is divided along a West-East axis, emanating into Europe and into Asia from the center of domestication in the Near East (Aradhya et al., 2003; Myles et al., 2011). Confounded with the geographic population structure in grape is also production use, in which wine grapes predominate in the West and table grapes in the East (Fig. 6). The genetic structure of the domesticated grape is in part determined by native wild *Vitis sylvestris* populations, with which local grape cultivars have outcrossed (Myles et al., 2011). To explore which traits most closely follow the domestication history, population structure, and local outcrossing in grape, we correlated traits with previously described PCs describing genetic structure ("genoPCs"; Supplemental Data Set S11).

After multiple test adjustment, only a small subset of leaf shape and GRIN traits correlate with genoPCs, mostly genoPC1 and genoPC3 (Supplemental Table S1; Supplemental Data Set S12). These traits exclusively belong to the aforementioned complex of hirsuteness, lobing and serration, and angular vein position traits (Supplemental Table S1; Figs. 5B and 7, A, B, and E). That these traits significantly correlate with genoPCs describing a West-to-East continuum of population structure (genoPC1; Figs. 6 and 7D) or a Near East versus West-and-East pattern of genetic diversity (genoPC3; Figs. 6 and 7G) demonstrates that this constellation of traits closely follows the domestication history and production uses of grape.

As native *V. sylvestris* populations influence the genetic structure of grape, an intriguing hypothesis is that wild populations altered the phenotype of domesticated grape through introgression. Consistent with this idea, for those traits that correlate with categorical classifications (Supplemental Table S2; Supplemental Data Set S13) of production use (iPC3; Fig. 7C) or geography (AR; Fig. 7F), the phenotype of western/wine grapes closely matches the phenotype of *V. sylvestris* accessions sampled from a population in Tunisia (DVIT2426). It should be noted that this population exhibits other ambiguous grape traits, such as green berries, perhaps indicating hybridization or a feral relationship with a local grape. Phenotypic and genotypic sampling of more *V. sylvestris* populations is required to confirm a phenotypic association of grape populations with local *V. sylvestris*. If demonstrated, it would suggest that the local domestication of grape cultivars was in part fueled through the introgression of potentially adaptive traits from native *V. sylvestris* populations.

Gene Expression Changes and Candidate Loci Regulating Leaf Shape

Extensive knowledge of gene regulatory networks responsible for patterning leaves exists in model organisms (Barkoulas et al., 2007; Husbands et al., 2009). However, examples of natural variation modulating leaf shape and the quantitative genetic basis of complex leaf morphologies remain scarce (Langlade et al., 2005; Tian et al., 2011; Chitwood et al., 2013). To understand the developmental pathways regulating complex leaf shapes, we performed RNA-Seq analysis on apices of Chasselas Dore (DVIT0689) and Chasselas Ciotat (DVIT0372) growing shoot tips (Supplemental Data Set S14). These two varieties are clonally related (Myles et al., 2011), and it has been speculated that Chasselas Ciotat may have arisen from Chasselas Dore as a spontaneous mutant event. Despite their clonal relationship, these varieties exhibit disparate morphologies (Fig. 1), to the extent that Chasselas Ciotat technically bears complex leaves.

Figure 7. (*Continued.*)
geography as a box plot, and a colored map indicates average trait values for accessions by country of origin. Note that for iPC3, the Tunisian accession sampled (DVIT2426; indicated by asterisks in the box plots and maps) has trait values resembling those for wine grapes, which predominately occupy western Europe near Tunisia. iPC3 values decrease West to East, reflecting the correlation with genoPC1. Similarly, the AR of the Tunisian accession's leaves resembles that of western cultivars, and the lowest ARs are found in leaves from central accessions, reflecting the central-specific pattern of genotypic variance explained by genoPC3 with which AR correlates.

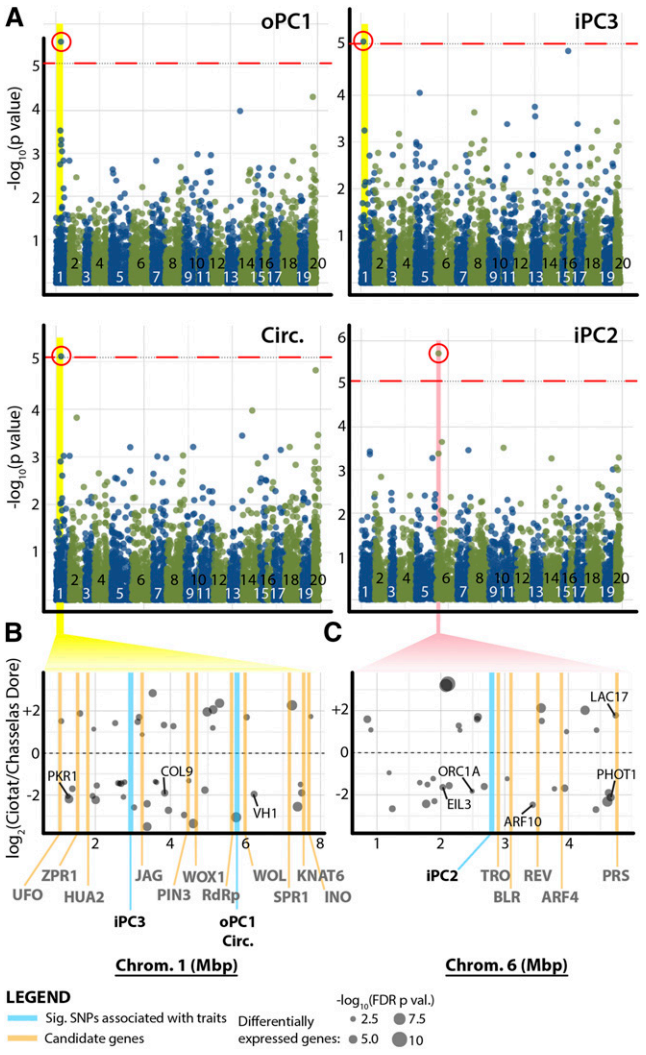

Figure 8. GWAS mapping of leaf traits. A, Significant associations between genetic markers measured by Myles et al. (2011) and leaf traits as determined using EMMAX (Kang et al., 2008) are shown. Negative log-transformed *P* values, indicated in blue and green for alternating chromosomes, are shown across the length of the genome with a Bonferroni-corrected *P* value threshold (0.05) indicated as a dotted red line. oPC1 and circularity significantly associate with the same polymorphism on chromosome 1. iPC3 associates with a nearby marker on chromosome 1, and iPC2 associates with a marker on chromosome 6. B, Expanded view of the yellow highlighted regions in A, showing significantly associated markers with iPC3, oPC1, and circularity on chromosome 1 (blue lines). Orange lines indicate homologs regulating leaf development within 2 Mb in either direction (names in gray below graph). Positions of differentially expressed genes between Chasselas Ciotat and Chasselas Dore and their $\log_2$ fold change values (*y* axis) are indicated by points (size proportional to significance). C, Similar to B, showing the expanded view of the pink highlighted region in A for the SNP associated with iPC2.

The 2,977 genes significantly (false discovery rate [FDR] < 0.05) down-regulated in the shoot apex of Chasselas Ciotat compared with Chasselas Dore (Supplemental Data Set S14) are enriched for Gene Ontology (GO) terms related to transcription, DNA binding, and nuclear localization (Supplemental Data Set S15). Underlying these GO terms are key developmental regulators of meristem identity and leaf patterning (Supplemental Data Set S16). Included are floral meristem (AGAMOUS-LIKE homologs), auxin (AUXIN-RESPONSE FACTOR homologs), cytokinin (HISTIDINE KINASE and RESPONSE REGULATOR homologs), RNA interference (ARGONAUTEs and DICER-LIKEs), and epigenetic (CHROMATIN REMODELING homologs) regulators as well as homeobox genes (ARABIDOPSIS THALIANA HOMEOBOX, BEL1-LIKE HOMEODOMAIN, and KNOTTED-LIKE HOMEOBOX homologs) and NAC domain transcripts. Interestingly, beyond these overt regulators of shoot apical meristem development, light regulation genes (including PHYTOCHROME, PHYTOCHROME-INTERACTING FACTOR, PHYTOCHROME-INTERACTING FACTOR-LIKE, and SUPPRESSOR OF PHYA homologs) are down-regulated in Chasselas Ciotat.

Contrastingly, the genes significantly up-regulated (2,370 genes; FDR < 0.05) in Ciotat versus Chasselas Dore (Supplemental Data Set S14) are enriched for GO terms concerning energy metabolism, mitochondria, electron transport, translation, cell wall modifications, and microtubules (Supplemental Data Set S17). A preponderance of ribosomal protein transcripts, cytochromes, hydrolases, cation/H^+ exchangers, and tubulin and microtubule-regulating factors comprise these genes (Supplemental Data Set S18). Given the connection between oxidative stress and leaf senescence (Gepstein et al., 2003; Woo et al., 2004), our results suggest that, associated with the complex leafed phenotype of Chasselas Ciotat, meristem identity and leaf-patterning pathways are down-regulated as leaf differentiation and senescence are promoted.

Gene expression analysis informs about gene regulatory networks contributing toward extreme phenotypes in a few varieties, but what are the polymorphisms governing leaf morphology throughout domesticated grape? We performed a GWAS for our traits using genotypic information (representing more than 5,000 single-nucleotide polymorphisms [SNPs]) previously collected on the vines used in this study (Myles et al., 2011). After multiple test adjustment, only a handful of SNPs remain significantly associated with circularity, oPC1, iPC3, and iPC2 (Fig. 8; Supplemental Data Set S19). Circularity, oPC1, and iPC3, a constellation of traits describing lobing and the descended petiolar junction of highly lobed varieties (Figs. 1 and 3), are associated with a single region on chromosome 1 spanning approximately 2.8 Mb (Fig. 8A). iPC2 (Fig. 3B) is associated with a marker on chromosome 6 (Fig. 8A). Around both of these loci are numerous known regulators of leaf development, and genes differentially expressed between Chasselas Ciotat and Chasselas Dore can also be superimposed on these regions (Fig. 8, B and C). Considering the high heritability of our traits (Table I), further development of genotyping resources in *Vitis* spp. (i.e. genome resequencing), phenotypic analysis of segregating populations, and sufficiently powered GWAS

studies may resolve loci regulating leaf shape in the future (Myles et al., 2011).

DISCUSSION

Our results attest to a strong genetic basis underlying the intricate phenotypes measured in this work and previously by ampelographers (Galet, 1952; Fig. 4). A large percentage of leaf shape and venation patterning exhibits high heritability (Figs. 1–3; Table I). Interestingly, complex shape phenotypes correlate with epidermal features, such as hirsuteness, and reproductive traits, revealing that disparate, potentially adaptive and economically relevant phenotypes cosegregate (Fig. 5). Leaf morphology also correlates with population structure, geography, and production use (Figs. 6 and 7), and gene expression analysis reveals that modulation of conserved pathways regulating shoot apical meristem development affect leaf shape in domesticated grape. What are the functional implications of the diverse leaf morphologies present in grape, and given the genetic basis of leaf shape, can it be practically used, through breeding or transgenics?

The cordate-shaped leaves of lianas, such as grape, have been hypothesized to play structural roles by balancing the blade atop the petiole (like a cantilever) to allow light foraging through leaf positioning (Givnish and Vermeij, 1976). In grapes, leaves are diurnally positioned to avoid excessive photon flux density (Gamon and Pearcy, 1989). Lobing, dissection, and serration in grape leaves are important for light to penetrate the canopy, mitigating not only the establishment of fungal infections (Spotts, 1977; Lalancette et al., 1988; Boso et al., 2010; Austin et al., 2011; Austin and Wilcox, 2012) but influencing cluster development and berry composition (Crippen and Morrison, 1986; Hunter et al., 1991; Morrison and Noble, 1990). Trichome density varies immensely in grape leaves, not only protecting against pathogens but providing photoprotection of the photosynthetic apparatus (Liakopoulos et al., 2006), thermoregulation, and boundary layer maintenance. Similarly, the patterning of veins and their distance to laminar mesophyll influences hydraulic efficiency and photosynthetic performance (Brodribb et al., 2007; Sack and Scoffoni, 2013).

The functional significance of leaves is timely, as environmental factors that climate change will alter have been demonstrated to affect vines via leaves. Increases in CO_2 concentration increase photosynthetic rates, yield, and water use efficiency through changes in leaf morphology, increased thickness, cell size, and decreased stomatal density (Moutinho-Pereira et al., 2009; Rogiers et al., 2011). Elevated CO_2 disproportionately affects vegetative traits over reproductive traits, and the increased leaf area and partial stomatal closure it causes has important consequences with respect to thermoregulation as well as water and canopy management (Bindi et al., 1996a, 1996b). Despite seemingly favorable physiological changes in response to increases in CO_2 concentration, grape yield and quality are expected to suffer when other climate change variables are considered. Increased UV-B radiation decreases leaf expansion, total biomass, and photosynthetic capacity and modulates leaf flavonoid and phenolic concentrations (Tevini and Teramura, 1989; Krupa and Jäger, 1996; Jansen et al., 1998; Schultz et al., 1998; Schultz, 2000; Kolb et al., 2001). Regions may become inhospitable to certain vines, in a manner mainly determined by latitude and temperature (Jackson and Cherry, 1988), decoupling combinations of temperature, soil types, topography, and cultivation that terroir attempts to preserve. Anticipated increases in temperature are predicted to shift the boundaries of European viticulture northward as much as 10 to 30 km per decade (Kenny and Harrison, 1993) and to reduce premium wine grape production in the United States by up to 81% (White et al., 2006). Recent studies confirm predictions of substantial climate change effects on viticulture (Hannah et al., 2013), although the degree of mitigation resulting from breeding, cultivation, and marketing innovations is debated (van Leeuwen et al., 2013).

Changes in leaf morphology with respect to changing climate are not unprecedented, as is apparent in the fossil record. Larger, entire leaves predominated in historically wetter, warmer climates, whereas smaller, more dissected leaves were common in cooler, drier climates (Bailey and Sinnott, 1915; Wolfe, 1971; Greenwood, 1992; Wilf et al., 1998; Chitwood et al., 2012a; Sack et al., 2012). Similarly, venation patterning functionally varies with climate and paleohistory as well (Sack and Scoffoni, 2013). Just as leaf morphology has changed over geologic time, breeding could be used to change grape leaf morphology in the coming decades to help mitigate the negative influences of climate change on viticulture, given (1) the tremendous natural variation in grape leaves and (2) its strong genetic basis. Once descriptive, the art and science of ampelography, combined with quantitative genetics and physiological studies, can potentially enhance and preserve viticultural traditions.

MATERIALS AND METHODS

Plant Materials and Photography

Photographs of leaves were collected from grapevines (*Vitis* spp.) maintained by the USDA National Clonal Germplasm Repository in Winters, California. More than 9,500 leaves were collected from more than 1,200 different domesticated grape (*Vitis vinifera*) varieties from May 28 through June 1, 2011. Most varieties were represented by two clonal vines, from which four leaves were sampled from each (such that eight leaves were sampled from most varieties). If possible, consecutive leaves of similar developmental stage were sampled from the midpoints of two shoots on each vine. All leaves were fully expanded but not so old that they had begun to senesce. Each day, vines were randomly sampled from the overall population. Samples were collected before noon, placed into Ziploc bags, and placed into a cooler. Leaves remained in the cooler in a 4°C cold room for a maximum of 48 h before being photographed.

Leaves were arranged under nonreflective glass over a light box (FB-WLT-1417; Fisher Scientific) so that veins (for Procrustes analysis) were clearly visible. Olympus SP-500 UZ cameras were mounted on copy stands (Adorama; 36-inch Deluxe Copy Stand) and controlled remotely by computer using Cam2Com software (Sabsik). A total of 4,950 raw photographs, with the file name indicating the vineyard position that can be used to identify the genotype (Supplemental Data Set S2), are available for download at www.chitwoodlab.org.

Morphometric Analyses

Using custom ImageJ (Abramoff et al., 2004) macros, individual leaves were extracted as binary images and named appropriately. For those leaves in which sinus regions were occluded by lobing, a small line was manually drawn to more accurately sample the overall outline of leaves. Leaf outlines were then batch processed in ImageJ to measure circularity, solidity, AR, and roundness.

Global analysis of leaf shape was conducted using EFDs followed by principal component analysis (PCA) using the program SHAPE (Iwata and Ukai, 2002). Object contours were extracted as chain code. Chain code was subsequently used to calculate normalized EFDs. Normalization was based upon manual orientation with respect to the proximal-distal axis of the leaf. PCA was performed on the EFDs resulting from the first 20 harmonics of Fourier coefficients. Coefficients of EFDs were calculated at −2 and +2 SD for each PC, and the respective contour shapes were reconstructed from an inverse Fourier transformation.

Original raw images were used for GPA to identify vein branch points, sinus valleys, and lobe tips. As described in the text, landmarks were placed on lobe tips, sinuses, and the petiolar junction for the outer analysis and on major vein branch points and the petiolar junction for the inner analysis. The x and y coordinates were collected using custom macros in ImageJ (Abramoff et al., 2004), and the GPA was performed and the resulting PCA scores were retrieved in R (R Core Team, 2013) using the "shapes" package (Dryden, 2013) with the procGPA() and shapepca() functions.

Correlational Analyses

Morphometric traits were correlated with (1) each other, (2) trait measurements made by Galet (1952), (3) phenotypes present in GRIN, (4) genotypic PCs, or (5) geography and/or production use. For the analysis with the traits measured by Galet (1952), 122 accessions were analyzed for which definitive matches by name could be made (Supplemental Data Set S5). GRIN traits were retrieved from http://www.ars-grin.gov/cgi-bin/npgs/html/crop.pl?273. Seventy-five traits, measured over multiple years, were considered (36 distinct traits). At minimum, each trait had values for 117 accessions represented in the USDA germplasm collection (Supplemental Data Set S8). Genotypic PCs, geographical information, and production use are derived from Myles et al. (2011) for 606 different accessions (Supplemental Data Set S11).

Correlation matrices were calculated using the rcorr() function from the Hmisc package (Harrell and Dupont, 2013) with appropriate multiple test adjustments using the p.adjust() function in R (R Core Team, 2013). For categorical variables (such as geography or production use), Kruskal-Wallis tests using the kruskal.test() function were used instead of correlation. Hierarchical clustering was performed using the hclust() function. Results were visualized using the ggplot2 package (Wickham, 2009).

Calculation of Heritability

Heritability was calculated by using the genotype data from Myles et al. (2011) combined with the phenotype data collected in this study. Genotype data were available for 961 phenotyped accessions and included 4,015 SNPs after removing SNPs with more than 20% missing data and minor allele frequencies < 0.01. The heritability of each trait was estimated using the method of Yang et al. (2011). Briefly, the total variance explained (PVE) was estimated using a single genetic relationship matrix and the variance due to population structure and cryptic relatedness (PVE.PS) was estimated using the SNP counts per chromosome in the regression model. The heritability of each trait was then calculated as $h^2 = \text{PVE} - \text{PVE.PS}$.

Genome-Wide Association

If the phenotype scores were not normally distributed (Shapiro test, $P < 0.05$), then the scores were transformed using the "boxcox" function in the MASS package in R (Venables and Ripley, 2002; R Core Team, 2013). The parameter of the Box-Cox power transformation, lambda, was chosen by choosing the value of lambda (from −10 to 10) that produced the maximum log likelihood. Genotype data were available for 961 phenotyped accessions and included 6,114 high-quality SNPs from the Vitis9KSNP array (Myles et al., 2011). GWAS was performed using the mixed model (Yu et al., 2006) implemented in EMMAX (Kang et al., 2010) with the identity-by-state matrix from PLINK (Purcell et al., 2007) as a random effect.

RNA-Seq Mapping and Differential Expression Analysis

RNA-Seq libraries were prepared using previously described methods (Kumar et al., 2012). RNA-Seq reads were preprocessed to remove low-quality reads (phred score < 20) and adapter contamination using the FastX toolkit (http://hannonlab.cshl.edu/fastx_toolkit/) and custom perl scripts. Quality-filtered reads from individual libraries (three replicates of each variety) were mapped to the domesticated grape reference transcript database (downloaded from ftp://ftp.jgi-psf.org/pub/compgen/phytozome/v9.0/Vvinifera/annotation/) using Burrows-Wheeler Aligner (BWA; parameters: bwa aln -k 1 -l 25 -n 0.04 -e 15 -i 10 and bwa samse -n 0; Li and Durbin, 2009), and only uniquely mapped reads were retained using custom perl script for downstream differential expression analysis. Uniquely mapped read counts for each gene were filtered using the Bioconductor package EdgeR version 3.2.3 such that only genes that have more than two reads per million in at least three of the samples were kept. Filtered read counts were normalized using the trimmed mean of M-values method followed by differential gene expression analysis between two varieties using classic pairwise comparison of EdgeR version 3.2.3 (Robinson and Oshlack, 2010).

RNA-Seq reads from this article can be found in Dryad under the DOI 10.5061/dryad.4d786.

Supplemental Data

The following materials are available in the online version of this article.

Supplemental Figure S1. Detailed hierarchical clustering of leaf and GRIN traits.

Supplemental Table S1. Traits significantly correlated with genotypic PCs.

Supplemental Table S2. Traits significantly correlated with geography and production use.

Supplemental Data Set S1. Trait values for accessions.

Supplemental Data Set S2. USDA germplasm collection accession information.

Supplemental Data Set S3. Leaf trait correlation.

Supplemental Data Set S4. Leaf trait correlation P values.

Supplemental Data Set S5. Measurements by Galet (1952).

Supplemental Data Set S6. Leaf and Galet (1952) trait correlation.

Supplemental Data Set S7. Leaf and Galet (1952) trait correlation P values.

Supplemental Data Set S8. GRIN and leaf trait values.

Supplemental Data Set S9. Leaf and GRIN trait correlation.

Supplemental Data Set S10. Leaf and GRIN trait correlation P values.

Supplemental Data Set S11. Genotypic PCA values and geographic point of origin and production type information.

Supplemental Data Set S12. Correlations between genotypic PCs with leaf traits and GRIN trichome density phenotypes.

Supplemental Data Set S13. Kruskal-Wallis tests between leaf traits and GRIN trichome density phenotypes with geographic and production type designations.

Supplemental Data Set S14. Differential gene expression between Chasselas Dore and Chasselas Ciotat.

Supplemental Data Set S15. GO terms significantly enriched for genes with increased expression in Chasselas Dore relative to Chasselas Ciotat.

Supplemental Data Set S16. Intersection between differentially expressed genes and enriched GO terms for genes up-regulated in Chasselas Dore.

Supplemental Data Set S17. GO terms significantly enriched for genes with increased expression in Chasselas Ciotat relative to Chasselas Dore.

Supplemental Data Set S18. Intersection between differentially expressed genes and enriched GO terms for genes up-regulated in Chasselas Ciotat.

Supplemental Data Set S19. Genome-wide association mapping results.

ACKNOWLEDGMENTS

We thank Peter Cousins for insightful discussions about the manuscript and natural variation among *Vitis* spp.

Received October 2, 2013; accepted November 25, 2013; published November 27, 2013.

LITERATURE CITED

Abramoff MD, Magalhaes PJ, Ram SJ (2004) Image processing with ImageJ. Biophotonics International **11:** 36–42

Aradhya MK, Dangl GS, Prins BH, Boursiquot JM, Walker MA, Meredith CP, Simon CJ (2003) Genetic structure and differentiation in cultivated grape, Vitis vinifera L. Genet Res **81:** 179–192

Austin CN, Grove GG, Meyers JM, Wilcox WF (2011) Powdery mildew severity as a function of canopy density: associated impacts on sunlight penetration and spray coverage. Am J Enol Vitic **62:** 23–31

Austin CN, Wilcox WF (2012) Effects of sunlight exposure on grapevine powdery mildew development. Phytopathology **102:** 857–866

Bailey IW, Sinnott EW (1915) A botanical index of Cretaceous and Tertiary climates. Science **41:** 831–834

Barkoulas M, Galinha C, Grigg SP, Tsiantis M (2007) From genes to shape: regulatory interactions in leaf development. Curr Opin Plant Biol **10:** 660–666

Bindi M, Fibbi L, Gozzini B, Orlandini S, Miglietta F (1996a) Modeling the impact of future climate scenarios on yield and yield variability of grapevine. Clim Res **7:** 213–224

Bindi M, Fibbi L, Gozzini B, Orlandini S, Seghi L (1996b) The effect of elevated CO_2 concentration on grapevine growth under field conditions. Acta Hortic **427:** 325–330

Boso S, Alonso-Villaverde V, Santiago JL, Gago P, Dürrenberger M, Düggelin M, Kassemeyer HH, Martinez MC (2010) Macro- and microscopic leaf characteristics of six grapevine genotypes (Vitis spp.) with different susceptibilities to grapevine downy mildew. Vitis **49:** 43–50

Brodribb TJ, Feild TS, Jordan GJ (2007) Leaf maximum photosynthetic rate and venation are linked by hydraulics. Plant Physiol **144:** 1890–1898

Chitwood DH, Headland LR, Filiault DL, Kumar R, Jiménez-Gómez JM, Schrager AV, Park DS, Peng J, Sinha NR, Maloof JN (2012a) Native environment modulates leaf size and response to simulated foliar shade across wild tomato species. PLoS ONE **7:** e29570

Chitwood DH, Headland LR, Kumar R, Peng J, Maloof JN, Sinha NR (2012b) The developmental trajectory of leaflet morphology in wild tomato species. Plant Physiol **158:** 1230–1240

Chitwood DH, Headland LR, Ranjan A, Martinez CC, Braybrook SA, Koenig DP, Kuhlemeier C, Smith RS, Sinha NR (2012c) Leaf asymmetry as a developmental constraint imposed by auxin-dependent phyllotactic patterning. Plant Cell **24:** 2318–2327

Chitwood DH, Kumar R, Headland LR, Ranjan A, Covington MF, Ichihashi Y, Fulop D, Jiménez-Gómez JM, Peng J, Maloof JN, et al (2013) A quantitative genetic basis for leaf morphology in a set of precisely defined tomato introgression lines. Plant Cell **25:** 2465–2481

Chitwood DH, Naylor DT, Thammapichai P, Weeger AC, Headland LR, Sinha NR (2012d) Conflict between intrinsic leaf asymmetry and phyllotaxis in the resupinate leaves of Alstroemeria psittacina. Front Plant Sci **3:** 182

Crippen DD, Morrison JC (1986) The effects of sun exposure on the compositional development of Cabernet Sauvignon berries. Am J Enol Vitic **37:** 235–242

Davies C, Robinson SP (1996) Sugar accumulation in grape berries: cloning of two putative vacuolar invertase cDNAs and their expression in grapevine tissues. Plant Physiol **111:** 275–283

Dengler N, Kang J (2001) Vascular patterning and leaf shape. Curr Opin Plant Biol **4:** 50–56

Dryden IL (2013) Shapes: Statistical Shape Analysis. R package version 1.1-8. http://CRAN.R-project.org/package=shapes (January 1, 2013)

Friedman WE, Diggle PK (2011) Charles Darwin and the origins of plant evolutionary developmental biology. Plant Cell **23:** 1194–1207

Galet P (1952) Précis d'Ampélographie Pratique. Impr. P. Déhan, Montpellier, France

Galet P (1979) A Practical Ampelography: Grapevine Identification. Translated by L Morton. Cornell University Press, Ithaca, NY

Gamon JA, Pearcy RW (1989) Leaf movement, stress avoidance and photosynthesis in Vitis californica. Oecologia **79:** 475–481

Gepstein S, Sabehi G, Carp MJ, Hajouj T, Nesher MF, Yariv I, Dor C, Bassani M (2003) Large-scale identification of leaf senescence-associated genes. Plant J **36:** 629–642

Givnish TJ, Vermeij GJ (1976) Sizes and shapes of liane leaves. Am Nat **110:** 743–778

Goethe JW (1817) Goethe's Werk, Italienische Reise. Dreizehnter Band, Stuttgart, Germany

Greenwood DR (1992) Taphonomic constraints on foliar physiognomic interpretations of Late Cretaceous and Tertiary palaeoclimates. Rev Palaeobot Palynol **71:** 149–190

Hannah L, Roehrdanz PR, Ikegami M, Shepard AV, Shaw MR, Tabor G, Zhi L, Marquet PA, Hijmans RJ (2013) Climate change, wine, and conservation. Proc Natl Acad Sci USA **110:** 6907–6912

Harrell FE, Dupont C (2013) Hmisc: Harrell Miscellaneous. R package version 3.10-1.1. http://CRAN.R-project.org/package=Hmisc (January 1, 2013)

Hunter JJ, De Villiers OT, Watts JE (1991) The effect of partial defoliation on quality characteristics of Vitis vinifera L. cv. Cabernet Sauvignon grapes. II. Skin color, skin sugar, and wine quality. Am J Enol Vitic **42:** 13–18

Husbands AY, Chitwood DH, Plavskin Y, Timmermans MC (2009) Signals and prepatterns: new insights into organ polarity in plants. Genes Dev **23:** 1986–1997

Iwata H, Niikura S, Matsuura S, Takano Y, Ukai Y (1998) Evaluation of variation of root shape of Japanese radish (Raphanus sativus L.) based on image analysis using elliptic Fourier descriptors. Euphytica **102:** 143–149

Iwata H, Ukai Y (2002) SHAPE: a computer program package for quantitative evaluation of biological shapes based on elliptic Fourier descriptors. J Hered **93:** 384–385

Jackson DI, Cherry NJ (1988) Prediction of a district's grape-ripening capacity using a latitude-temperature index (LTI). Am J Enol Vitic **39:** 19–28

Jansen MAK, Gaba V, Greenberg B (1998) Higher plants and UV-B radiation: balancing damage, repair, and acclimation. Trends Plant Sci **4:** 131–135

Kang HM, Sul JH, Service SK, Zaitlen NA, Kong SY, Freimer NB, Sabatti C, Eskin E (2010) Variance component model to account for sample structure in genome-wide association studies. Nat Genet **42:** 348–354

Kang HM, Zaitlen NA, Wade CM, Kirby A, Heckerman D, Daly MJ, Eskin E (2008) Efficient control of population structure in model organism association mapping. Genetics **178:** 1709–1723

Kenny GH, Harrison PA (1993) The effects of climatic variability and change on grape suitability in Europe. J Wine Res **4:** 163–183

Koenig D, Bayer E, Kang J, Kuhlemeier C, Sinha N (2009) Auxin patterns Solanum lycopersicum leaf morphogenesis. Development **136:** 2997–3006

Kolb CA, Käser MA, Kopecký J, Zotz G, Riederer M, Pfündel EE (2001) Effects of natural intensities of visible and ultraviolet radiation on epidermal ultraviolet screening and photosynthesis in grape leaves. Plant Physiol **127:** 863–875

Krupa SV, Jäger HJ (1996) Adverse effects of elevated levels of ultraviolet (UV)-B radiation and ozone (O_3) on crop growth and productivity. *In* F Bazzaz, W Sombroek, eds, Global Climate Change and Agricultural Production. John Wiley & Sons, Chichester, UK, pp 141–169

Kumar R, Ichihashi Y, Kimura S, Chitwood DH, Headland LR, Peng J, Maloof JN, Sinha NR (2012) A high-throughput method for Illumina RNA-Seq library preparation. Front Plant Sci **3:** 202

Lalancette N, Madden LV, Ellis MA (1988) A quantitative model for describing the sporulation of Plasmopara viticola on grape leaves. Phytopathology **78:** 1316–1321

Langlade NB, Feng X, Dransfield T, Copsey L, Hanna AI, Thébaud C, Bangham A, Hudson A, Coen E (2005) Evolution through genetically controlled allometry space. Proc Natl Acad Sci USA **102:** 10221–10226

Li H, Durbin R (2009) Fast and accurate short read alignment with Burrows-Wheeler transform. Bioinformatics **25:** 1754–1760

Liakopoulos G, Nikolopoulos D, Klouvatou A, Vekkos KA, Manetas Y, Karabourniotis G (2006) The photoprotective role of epidermal anthocyanins and surface pubescence in young leaves of grapevine (Vitis vinifera). Ann Bot (Lond) **98:** 257–265

McLellan T (2005) Correlated evolution of leaf shape and trichomes in *Begonia dregei* (Begoniaceae). Am J Bot **92:** 1616–1623

Morrison JC, Noble AC (1990) The effects of leaf and cluster shading on the composition of Cabernet Sauvignon grapes and on fruit and wine sensory properties. Am J Enol Vitic **41:** 193–200

Moutinho-Pereira J, Goncalves B, Bacelar E, Cunha JB, Coutinho J, Correia CM (2009) Effects of elevated CO_2 on grapevine (*Vitis vinifera* L.): physiological and yield attributes. Vitis **48:** 159–165

Mullins MG, Bouquet A, Williams LE (1992) Biology of the grapevine. *In* Biology of Horticultural Crops. Cambridge University Press, Cambridge, UK, pp 33–34

Myles S, Boyko AR, Owens CL, Brown PJ, Grassi F, Aradhya MK, Prins B, Reynolds A, Chia JM, Ware D, et al (2011) Genetic structure and domestication history of the grape. Proc Natl Acad Sci USA **108:** 3530–3535

Purcell S, Neale B, Todd-Brown K, Thomas L, Ferreira MA, Bender D, Maller J, Sklar P, de Bakker PI, Daly MJ, et al (2007) PLINK: a tool set for whole-genome association and population-based linkage analyses. Am J Hum Genet **81:** 559–575

R Core Team (2013) R: A Language and Environment for Statistical Computing. R Foundation for Statistical Computing, Vienna, Austria, http://www.R-project.org/ (January 1, 2013)

Reinhardt D, Pesce ER, Stieger P, Mandel T, Baltensperger K, Bennett M, Traas J, Friml J, Kuhlemeier C (2003) Regulation of phyllotaxis by polar auxin transport. Nature **426:** 255–260

Robinson MD, Oshlack A (2010) A scaling normalization method for differential expression analysis of RNA-seq data. Genome Biol **11:** R25

Rogiers SY, Hardie WJ, Smith JP (2011) Stomatal density of grapevine leaves (*Vitis vinifera* L.) responds to soil temperature and atmospheric carbon dioxide. Aust J Grape Wine Res **17:** 147–152

Rohlf FJ, Slice DE (1990) Extensions of the Procrustes method for the optimal superimposition of landmarks. Syst Zool **39:** 40–59

Sack L, Scoffoni C (2013) Leaf venation: structure, function, development, evolution, ecology and applications in the past, present and future. New Phytol **198:** 983–1000

Sack L, Scoffoni C, McKown AD, Frole K, Rawls M, Havran JC, Tran H, Tran T (2012) Developmentally based scaling of leaf venation architecture explains global ecological patterns. Nat Commun **3:** 837

Scarpella E, Marcos D, Friml J, Berleth T (2006) Control of leaf vascular patterning by polar auxin transport. Genes Dev **20:** 1015–1027

Schultz HR (2000) Climate change and viticulture: a European perspective on climatology, carbon dioxide and UV-B effects. Aust J Grape Wine Res **6:** 2–12

Schultz HR, Löhnertz O, Bettner W, Bálo B, Linsenmeier A, Jähnisch A, Müller M, Gaubatz B, Váradi G (1998) Is grape composition affected by current levels of UV-B radiation? Vitis **37:** 191–192

Spotts RA (1977) Effect of leaf wetness duration and temperature on the infectivity of Guignardia bidwellii on grape leaves. Phytopathology **67:** 1378–1381

Tevini M, Teramura AH (1989) UV-B effects on terrestrial plants. Photochem Photobiol **50:** 479–487

Tian F, Bradbury PJ, Brown PJ, Hung H, Sun Q, Flint-Garcia S, Rocheford TR, McMullen MD, Holland JB, Buckler ES (2011) Genome-wide association study of leaf architecture in the maize nested association mapping population. Nat Genet **43:** 159–162

van Leeuwen C, Schultz HR, de Cortazar-Atauri IG, Duchene E, Ollat N, Pieri P, Bois B, Goutouly JP, Quenol H, Touzard JM, et al (2013) Why climate change will not dramatically decrease viticultural suitability in main wine-producing areas by 2050. Proc Natl Acad Sci USA **110:** E3051–3052

Venables WN, Ripley BD (2002) Modern Applied Statistics with S, Ed 4. Springer, New York

Viscosi V, Cardini A (2011) Leaf morphology, taxonomy and geometric morphometrics: a simplified protocol for beginners. PLoS ONE **6:** e25630

White MA, Diffenbaugh NS, Jones GV, Pal JS, Giorgi F (2006) Extreme heat reduces and shifts United States premium wine production in the 21st century. Proc Natl Acad Sci USA **103:** 11217–11222

Wickham H (2009) ggplot2: Elegant Graphics for Data Analysis. Springer, New York

Wilf P, Wing SL, Greenwood DR, Greenwood CL (1998) Using fossil leaves as paleoprecipitation indicators: an Eocene example. Geology **26:** 203–206

Wolfe JA (1971) Tertiary climate fluctuations and methods of analysis of Tertiary floras. Palaeogeogr Palaeoclimatol Palaeoecol **9:** 27–57

Woo HR, Kim JH, Nam HG, Lim PO (2004) The delayed leaf senescence mutants of Arabidopsis, ore1, ore3, and ore9 are tolerant to oxidative stress. Plant Cell Physiol **45:** 923–932

Yang J, Manolio TA, Pasquale LR, Boerwinkle E, Caporaso N, Cunningham JM, de Andrade M, Feenstra B, Feingold E, Hayes MG, et al (2011) Genome partitioning of genetic variation for complex traits using common SNPs. Nat Genet **43:** 519–525

Yu J, Pressoir G, Briggs WH, Vroh Bi I, Yamasaki M, Doebley JF, McMullen MD, Gaut BS, Nielsen DM, Holland JB, et al (2006) A unified mixed-model method for association mapping that accounts for multiple levels of relatedness. Nat Genet **38:** 203–208